

# The origin of hyperferroelectricity in $\text{LiBO}_3$ ( $B=\text{V}, \text{Nb}, \text{Ta}, \text{Os}$ )

Pengfei Li,<sup>1,2</sup> Xinguo Ren,<sup>1,2</sup> Guang-Can Guo,<sup>1,2</sup> and Lixin He<sup>1,2,\*</sup>

<sup>1</sup>Key Laboratory of Quantum Information, University of Science and Technology of China, Hefei, 230026, China

<sup>2</sup>Synergetic Innovation Center of Quantum Information and Quantum Physics,  
University of Science and Technology of China, Hefei, 230026, China

(Dated: May 17, 2018)

The electronic and structural properties of  $\text{LiBO}_3$  ( $B=\text{V}, \text{Nb}, \text{Ta}, \text{Os}$ ) are investigated via first-principles methods. We show that  $\text{LiBO}_3$  belong to the recently proposed hyperferroelectrics, i.e., they all have unstable longitudinal optic phonon modes. Especially, the ferroelectric-like instability in the metal  $\text{LiOsO}_3$ , whose optical dielectric constant goes to infinity, is a limiting case of hyperferroelectrics. Via an effective Hamiltonian, we further show that, in contrast to normal proper ferroelectricity, in which the ferroelectric instability usually comes from long-range coulomb interactions, the hyperferroelectric instability is due to the structure instability driven by short-range interactions. This could happen in systems with large ion size mismatches, which therefore provides a useful guidance in searching for novel hyperferroelectrics.

PACS numbers: 77.80.-e, 77.22.Ej

The switchable polarization of ferroelectrics made them an important class of materials for modern device applications. However, in traditional proper ferroelectrics, the electric polarization is very sensitive to the domain wall structures and electric boundary conditions [1]. This is even more severe in the case of ferroelectric thin films [2, 3], where the depolarization field may easily destroy the polarization states. Recently in a seminal work [4], Garrity, Rabe and Vanderbilt (GRV) showed that a class of recently discovered hexagonal *ABC* semiconducting ferroelectrics [5] have very robust polarization properties even when the depolarization field is unscreened, e.g., can remain polarized down to single atomic layers when interfaced with normal insulators, therefore they are given the name of *hyperferroelectrics*. These properties are extremely important for modern device applications which utilize the ferroelectric thin films [6]. GRV further showed that the extraordinary behavior of hyperferroelectrics is because they have an unstable longitudinal optic (LO) mode besides the transverse optic (TO) mode instability.

It has been proposed that in the hexagonal *ABC* hyperferroelectrics, the imaginary LO phonon frequency is due to the small LO-TO splitting, which further arises from their small energy gaps – thus large optical dielectric constants  $\epsilon_\infty$  – as well as small Born effective charges [4]. However, in this Letter, we show that  $\text{LiNbO}_3$ ,  $\text{LiTaO}_3$  are also hyperferroelectrics, because they have unstable LO phonon modes as well, despite that they have relative small  $\epsilon_\infty$  and large mode effective charges, in contrast with the above-mentioned *ABC* hyperferroelectrics. This poses an interesting question: is there a more general (fundamental) driving mechanism for hyperferroelectrics, besides the small LO-TO splitting scenario disclosed by GRV for hexagonal *ABC* ferroelectrics? We will answer the question in this work using the  $\text{LiBO}_3$ -type materials.

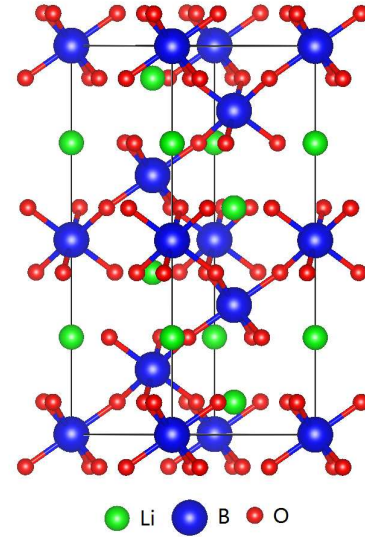


FIG. 1. (Color online) The hypothetical paraelectric (PE) structure of  $\text{LiBO}_3$  resulting from an average of the disordered structure above  $T_c$ .

$\text{LiNbO}_3$  and  $\text{LiTaO}_3$  are two important ferroelectrics which have been investigated intensively in the past years [7–12]. The ferroelectric transition of these materials is believed to be of order-disorder character. Shown in Fig. 1 is the hypothetical paraelectric (PE) structure of  $\text{LiBO}_3$  ( $B=\text{Nb}, \text{Ta}$ ), resulting from an average of the disordered structure above  $T_c$ . The paraelectric (PE) structure belongs to the  $R\bar{3}c$  space group, whereas the ferroelectric (FE) structure is rhombohedral, and belongs to the space group  $R3c$ . In the FE phase, the Li, O and B ions distort from their central symmetric positions, and induce the electric polarization along the trigonal axis. Inbar and Cohen studied the electronic and structural properties of  $\text{LiNbO}_3$  and  $\text{LiTaO}_3$  [12]. They

TABLE I. Calculated band gaps, optical dielectric constants and atomic Born effective charges of  $\text{LiBO}_3$ .

	gap (eV)	$\epsilon_\infty$	$Z_c^*(\text{Li})$	$Z_c^*(\text{B})$	$Z_c^*(\text{O})$
$\text{LiVO}_3$	0.4	18.8	1.13	13.36	-4.83
$\text{LiNbO}_3$	2.2	7.3	1.09	9.37	-3.49
$\text{LiTaO}_3$	3.0	5.8	1.10	8.36	-3.15
$\text{LiOsO}_3$	0	$\infty$			

found large hybridization between the transition-metal  $B$  atoms and the oxygen  $2p$  states, similar to perovskite ferroelectrics. It has thus been suggested that the ferroelectricity in  $\text{LiNbO}_3$  and  $\text{LiTaO}_3$  is due to long-range Coulomb interactions. Interestingly, very recently it has been found that  $\text{LiOsO}_3$ , even though being a metal, also has ferroelectric-like structural transitions [13]. It is very puzzling where the ferroelectric-like structure of  $\text{LiOsO}_3$  comes from, since the long-range Coulomb long-range interactions should be screened in the metallic states. The mechanism for the FE-like structural transition in metal is still under debate [14, 15].

In this Letter, we investigate the ferroelectric properties of  $\text{LiBO}_3$ -type compounds, where  $B=\text{V, Nb, Ta}$  and  $\text{Os}$ . We show that  $\text{LiBO}_3$  are hyperferroelectrics, and there are two co-existing and yet distinct ferroelectric mechanisms in  $\text{LiBO}_3$ , namely the long-range Coulomb interactions due to  $B$  ions, and short-range structural instability due to Li ions. Especially we show that the instability of Li ions is responsible for the hyperferroelectric behavior of  $\text{LiBO}_3$ . The FE-like structural transition in metallic  $\text{LiOsO}_3$  [13] is nothing special, but has the same mechanism of other  $\text{LiBO}_3$  compounds. In this sense,  $\text{LiOsO}_3$  can be viewed as a special hyperferroelectrics in the limit of  $\epsilon_\infty \rightarrow \infty$ . Via an effective Hamiltonian model, we further clarify that the microscopic origin of hyperferroelectrics is from the instability driven by short-range interactions. These results provide a strong guidance in searching for novel hyperferroelectrics.

The ferroelectric phase transitions can be understood by the lattice dynamics of their high-symmetry phase. For ferroelectrics, the high-symmetry phase has at least one unstable TO mode. The frequencies of TO can be calculated using first-principles methods in bulk materials in the absence of macroscopic electric field ( $E=0$ ) [4]. If the depolarization field is unscreened, corresponding to the case of electric displacement  $D=0$ , the structure instability is determined by the LO modes, which can be obtained by adding to the dynamic matrix a non-analytic long-range Coulomb term (known as the LO-TO splitting) [1, 16] that schematically takes the form  $4\pi Z^{*2}/\Omega\epsilon_\infty$ , where  $Z^*$  is the Born effective charge and  $\Omega$  is the volume of unit cell. In normal ferroelectrics, such as  $\text{PbTiO}_3$ ,  $\text{BaTiO}_3$ , etc., due to their large Born effective charges and relatively small  $\epsilon_\infty$ , the LO-TO splittings are huge, such that all LO modes are stable [1]. Therefore

they lose ferroelectricity if the depolarization field is not well screened. In contrast, in the  $ABC$  hexagonal hyperferroelectrics (e.g.,  $\text{LiZnAs}$ ) as discussed by GRV [4], the LO-TO splittings are small, such that even the LO modes can become unstable. Consequently, the polarization in these materials is very robust against the depolarization field.

Ferroelectric materials with small LO-TO splittings are the most obvious candidates for hyperferroelectrics. Therefore, it is a natural attempt to look for the hyperferroelectrics in materials with (i) small band gap, or equivalently large electronic dielectric constant  $\epsilon_\infty$ ; (ii) small mode effective charges. Indeed, the hyperferroelectrics found by GRV all satisfy these conditions [4]. However, as demonstrated below,  $\text{LiNbO}_3$  and  $\text{LiTaO}_3$  are also hyperferroelectrics, i.e., having unstable LO phonon modes, despite that they have large band gap, relatively small optical dielectric constants, and large effective mode effective charges.

The electronic and structural properties of  $\text{LiBO}_3$  are calculated using density functional theory within local density approximation (LDA), implemented in the Vienna ab initio simulations package (VASP) [17, 18]. The projector augmented-wave (PAW) pseudopotentials [19] with a 500 eV plane-wave cutoff are used. The Brillouin zone is sampled with a  $8\times 8\times 8$  Monkhorst-Pack k-point grid converges the results very well. We relax the structure until the remaining forces are less than 1 meV/Å. Phonon frequencies are calculated using a finite difference method as implemented in Phonopy package [20]. The Born effective charges and the optical dielectric constants are calculated using density functional perturbation theory (DFPT) [21]. The above properties of  $\text{LiBO}_3$  are also calculated using other functionals, including GGA and LDA+U. Although the exact numbers of the results may vary, the main conclusions are remain unchanged.

The calculated band gaps (via DFT-LDA) of  $\text{LiBO}_3$  are listed in Table I for their paraelectric states. We see that the LDA calculated band gaps of  $\text{LiNbO}_3$  and  $\text{LiTaO}_3$  are 2.2 and 3.0 eV respectively (which surprisingly are not much underestimated compared to the experimental values [22, 23]). The band gaps are comparable to those of perovskite ferroelectrics, much larger than the band gaps of  $ABC$  hexagonal hyperferroelectrics, which are around 0.5 - 1 eV [4].  $\text{LiVO}_3$  has relative small LDA band gap, which is approximately 0.4 eV.  $\text{LiOsO}_3$  is a metal [13]. The calculated optical dielectric constant  $\epsilon_\infty^{zz}$  along the (polar)  $z$  axis and Born effective charges are also listed in Table I. We see that  $\text{LiNbO}_3$  and  $\text{LiTaO}_3$  have  $\epsilon_\infty^{zz}$  approximately 5 -7, similar to those of perovskite ferroelectrics, e.g.,  $\text{PbTiO}_3$ ,  $\text{BaTiO}_3$ . The dielectric constant of  $\text{LiVO}_3$  is somehow larger, approximately 19, consistent with the fact that  $\text{LiVO}_3$  has smaller band gap.  $\text{LiOsO}_3$  is a metal, and therefore its  $\epsilon_\infty^{zz}$  diverges. We then calculate the atomic Born effective charges for  $\text{LiVO}_3$ ,  $\text{LiNbO}_3$  and  $\text{LiTaO}_3$ . The effective charge of Li

TABLE II. Calculated phonon frequencies of the softest TO modes ( $\omega_{TO}$ ), LO modes ( $\omega_{LO}$ ) and the phonon modes due to pure short-range interactions [ $\omega_s$ , calculated using Eq. (8)]. Also shown are the mode effective charges  $Z_{TO}^*$  of the TO modes, and the electric polarization under  $E=0$  and  $D=0$ . The values for  $\text{PbTiO}_3$ ,  $\text{BaTiO}_3$ ,  $\text{NaNbO}_3$ , and  $\text{KNbO}_3$  are obtained under their cubic structures.

	$\omega_{TO}$ ( $\text{cm}^{-1}$ )	$\omega_{LO}$ ( $\text{cm}^{-1}$ )	$\omega_s$ ( $\text{cm}^{-1}$ )	$Z_{TO}^*$	$P_{E=0}$ ( $\text{C/m}^2$ )	$P_{D=0}$ ( $\text{C/m}^2$ )
$\text{LiVO}_3$	409 <i>i</i>	160 <i>i</i>	160 <i>i</i>	20.1	1.79	0.29
$\text{LiNbO}_3$	208 <i>i</i>	104 <i>i</i>	125 <i>i</i>	8.9	1.00	0.08
$\text{LiTaO}_3$	188 <i>i</i>	77 <i>i</i>	110 <i>i</i>	5.8	0.72	0.05
$\text{LiOsO}_3$	183 <i>i</i>	183 <i>i</i>	183 <i>i</i>	-	-	-
$\text{PbTiO}_3$	119 <i>i</i>	105	95	7.5	0.57	0
$\text{BaTiO}_3$	91 <i>i</i>	181	180	10.1	0.12	0
$\text{NaNbO}_3$	167 <i>i</i>	81	73	8.7	0.49	0
$\text{KNbO}_3$	143 <i>i</i>	172	171	10.8	0.29	0

ions is approximately 1.0, suggesting that Li is totally ionized. The effective charges of V, Nb, and Ta ions are approximately 13, 9, and 8 respectively, which are anomalously larger than their valence electron charges, similar to those of perovskite ferroelectrics. It is usually believed that the anomalous effective charges introduce large long-range Coulomb interactions, leading to spontaneous electric polarization in ferroelectrics [12, 24].

To study the structure instabilities in  $\text{LiBO}_3$ , we calculate the phonons of  $\text{LiBO}_3$  at  $\Gamma$  point in the PE phases using a 10-atom unit cell. We focus on the  $A_{2u}$  modes which are associated with the ferroelectric structural transitions. For these modes, the phonon frequencies for both the TO mode and LO modes are calculated. The summary of the results are given in Table II. As a comparison, we also present the results for some normal perovskite ferroelectrics, including  $\text{PbTiO}_3$ ,  $\text{BaTiO}_3$ ,  $\text{NaNbO}_3$ , and  $\text{KNbO}_3$ . We note that the results for the perovskites are all obtained at their cubic structure. As listed in Table II,  $\text{LiVO}_3$ ,  $\text{LiNbO}_3$ ,  $\text{LiTaO}_3$ , and  $\text{LiOsO}_3$  all have very strong instable TO modes. This is consistent with the proposal that  $\text{LiTaO}_3$  and  $\text{LiNbO}_3$  are order-disorder ferroelectrics [7–11], in which the centrosymmetric structures have much higher energies than the distorted structures. The calculated mode effective charges for  $\text{LiVO}_3$ ,  $\text{LiNbO}_3$ , and  $\text{LiTaO}_3$  are approximately 20, 9, and 6, respectively. The Born effective charges are ill-defined for  $\text{LiOsO}_3$ , which is a metal. We also present the electric polarizations for their FE phase, which are comparable to those of perovskite ferroelectrics.

The LO phonon frequencies are calculated by diagonalizing the resultant matrix obtained by adding the non-analytic terms to the dynamic matrix, i.e.,

$$D_{ij}^{\text{LO}}(0) = D_{ij}^{\text{TO}}(0) + \frac{4\pi}{\Omega} \frac{Z_i^* Z_j^*}{\epsilon_\infty}, \quad (1)$$

where  $Z_i^*$ ,  $Z_j^*$  are the atomic effective charges. The re-

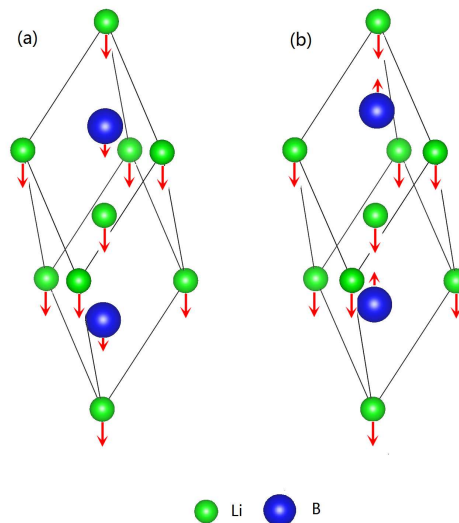


FIG. 2. (Color online) The schematic phonon patterns showing the atomic displacements of Li and B atoms for the soft (a) TO mode, and (b) LO mode. For clarity, we neglect the oxygen atoms.

sults are also given in Table II. Remarkably, all calculated  $\text{LiBO}_3$  compounds have soft LO modes, indicating that they are hyperferroelectrics, similar to the  $ABC$  hexagonal ferroelectrics but in contrast to the perovskite ones. For  $\text{LiOsO}_3$ , the TO modes and LO modes have the same frequencies, because its  $1/\epsilon_\infty=0$ . These results are quite surprising, given that the dielectric constants  $\epsilon_\infty$  of  $\text{LiNbO}_3$  and  $\text{LiTaO}_3$  are relative small, and the mode effective charges are quite large, similar to those of the traditional perovskite ferroelectrics, such as  $\text{PbTiO}_3$ ,  $\text{BaTiO}_3$  etc. One may expect that the LO-TO splitting  $4\pi Z^{*2}/\Omega\epsilon_\infty$  would stabilize all LO modes. To understand the origin of the soft  $A_{2u}$  modes of  $\text{LiBO}_3$ , for both TO modes and LO modes. The atomic displacements of the soft TO and LO phonons are shown in Fig. 2(a) and 2(b), respectively. In TO modes, Li ions and B ( $B=\text{V, Nb, Ta}$ ) ions move in the same direction, whereas the O ions (not shown) move along the opposite direction. The Li ions have the largest displacement, where B and O ions also have significant contributions. For LO modes, the displacements of O ions along the  $c$  axis are somehow suppressed. Surprisingly, the displacements of B ions reverse from those of the TO mode, i.e., opposite to the polarization direction! These results show that the phonon eigenvectors are very sensitive to the electric boundary conditions, and are very different for TO modes and LO modes. Therefore, adding the simple correction term  $4\pi Z^{*2}/\Omega\epsilon_\infty$  to the TO modes would significantly overestimate the LO-TO splitting, and falsely stabilizes all LO modes. One has to make the non-analytical corrections to the dynamic matrices themselves. As we see

from Eq. 1 the corrections to the V, Nb, Ta ions are very large due to their large effective charges; whereas the corrections for Li ions are small, because  $Z^*(\text{Li}) \approx 1$ , is small. Therefore, the LO modes of  $\text{LiBO}_3$  can remain soft by altering their mode patterns.

From the above analysis, one can see there are two co-existing ferroelectric mechanisms in  $\text{LiBO}_3$ . One is the long-range Coulomb interactions due to large Born effective charges arising from the B ions, which are very sensitive to the electric boundary conditions, just like normal proper ferroelectrics; the second is short-range instability due to the large size mismatch between the Li and B ions [14], which is robust against the electric boundary conditions. Especially for metallic  $\text{LiOsO}_3$ , the FE-like structural transition is induced by the short-range instability of Li alone, because the long-range Coulomb interactions is screened.

We also calculated the electric polarization under the condition  $D=0$  by using the model of Ref. [4], and the results are listed in Table II. As expected, for normal ferroelectrics  $\text{PbTiO}_3$ ,  $\text{BaTiO}_3$ ,  $\text{NaNbO}_3$ , and  $\text{KNbO}_3$ , the spontaneous polarizations are all zero under  $D=0$ . In contrast, for  $\text{LiVO}_3$ ,  $\text{LiNbO}_3$ , and  $\text{LiTaO}_3$ , the spontaneous polarizations under  $D=0$  are about one tenth of those under  $E=0$ , but still significant for applications. These results further confirm that they are hyperferroelectrics.

We have shown that the large electronic dielectric constant and small effective charges may not be the necessary condition for the hyperferroelectrics. This raises an interesting question: what are responsible for it? To answer this question, we start from a simplified effective Hamiltonian for ferroelectrics following Ref. [24],

$$E(\{\mathbf{u}_i\}) = E^{\text{dipol}}(\{\mathbf{u}_i\}) + E^{\text{self}}(\{\mathbf{u}_i\}) + E^{\text{short}}(\{\mathbf{u}_i\}), \quad (2)$$

where  $\mathbf{u}_i$  are the local normal modes at  $i$ -th cell.  $E^{\text{dipol}}$  represents the long-range dipole-dipole interaction, whereas  $E^{\text{self}}$ ,  $E^{\text{short}}$  are the energies of isolated local modes, and the short-range interactions between the local modes respectively. For the simplicity of discussion, we neglect the elastic energies, and their coupling to the local modes. Without losing generality, we further assume that the crystal has simple cubic structure.

First, let's look at the dipole-dipole interactions,

$$E^{\text{dipol}}(\{\mathbf{u}_i\}) = \frac{Z^{*2}}{\epsilon_\infty} \sum_{i < j} \frac{\mathbf{u}_i \cdot \mathbf{u}_j - 3(\hat{\mathbf{R}}_{ij} \cdot \mathbf{u}_i)(\hat{\mathbf{R}}_{ij} \cdot \mathbf{u}_j)}{R_{ij}^3}, \quad (3)$$

where  $\epsilon_\infty$  is the optical dielectric constant of the material.  $R_{ij}=|\mathbf{R}_{ij}|$  is the distance between the two local modes, where  $\mathbf{R}_{ij}=\mathbf{R}_i-\mathbf{R}_j$  and  $\hat{\mathbf{R}}_{ij}=\mathbf{R}_{ij}/R_{ij}$ . Direct evaluation of Eq. 3 in real space converges very slowly. Equation 3 can be evaluated using Ewald summation techniques. For simple cubic structure of infinite lattice size, the summation have been obtained in Ref.[25]. It turns out that

$E^{\text{dipol}}$  is non-analytic when  $\mathbf{q} \rightarrow 0$ ,

$$E^{\text{dipol}}(\{\mathbf{u}\}) = -\frac{2\pi}{3\Omega} \frac{Z^{*2}}{\epsilon_\infty} \left(1 - 3\frac{q_z^2}{|\mathbf{q}|^2}\right) u^2 \quad (4)$$

where  $u = |\mathbf{u}|$  and  $\Omega$  is the unit cell volume. Here, we assume that the phonon displacements are along the  $z$  axis. The short-range interactions can be obtained by setting  $Z^* \rightarrow 0$ , or  $\epsilon_\infty \rightarrow \infty$ . The self-energy and the energy due to short-range interactions can thus be written in the following form as  $\mathbf{q} \rightarrow 0$ ,

$$E^{\text{self}}(\{\mathbf{u}_i\}) + E^{\text{short}}(\{\mathbf{u}_i\}) = E_0 + \frac{1}{2}\omega_s^2 u^2 + \frac{1}{4}\kappa_4 u^4, \quad (5)$$

where  $\omega_s^2 = \kappa_2 + \frac{1}{2} \sum_{ij} J_{ij}$ ,  $\kappa_2$  is the on-site energy contribution, and  $J_{ij}$  are the coupling constants between local modes  $\mathbf{u}_i$  and  $\mathbf{u}_j$ . Therefore, the phonon frequency of the TO mode can be calculated as  $q_x, q_y \rightarrow 0$ ,

$$\omega_{TO}^2 = \omega_s^2 - \frac{4\pi}{3\Omega} \frac{Z^{*2}}{\epsilon_\infty}, \quad (6)$$

and the phonon frequencies of LO modes can be obtained as,

$$\omega_{LO}^2 = \omega_s^2 + \frac{8\pi}{3\Omega} \frac{Z^{*2}}{\epsilon_\infty}, \quad (7)$$

i.e.,  $\omega_{LO}^2 = \omega_{TO}^2 + \frac{4\pi}{\Omega} \frac{Z^{*2}}{\epsilon_\infty}$ . Assuming that the eigenvectors of LO modes do not change much from that of TO modes, we can estimate  $\omega_s^2 = (2\omega_{TO}^2 + \omega_{LO}^2)/3$ . More generally,  $\omega_s^2$  can be obtained by solving the following dynamic matrix,

$$D_{ij}^s(0) = D_{ij}^{\text{TO}}(0) + \frac{4\pi}{3\Omega} \frac{Z_i^* Z_j^*}{\epsilon_\infty}. \quad (8)$$

We list the softest  $\omega_s$  for typical perovskite ferroelectrics as well as  $\text{LiBO}_3$ , in Table II. As we can see from the Table, in traditional perovskite ferroelectrics, such as  $\text{PbTiO}_3$ ,  $\text{BaTiO}_3$  etc.,  $\omega_s$  are all stable, meaning that the short-range interactions favorite the high symmetry non-polar structures. However, because of the large Born effective charges and small optical dielectric constants  $\epsilon_\infty$  in these materials, the long-range Coulomb interactions (the second term in the right hand of Eq. 6) overcome the short-range repulsive interactions  $\omega_s^2$ , and the TO phonon mode frequencies become soft. In these materials, LO modes  $\omega_{LO}^2$  are all positive because  $\omega_s^2$  are already positive. These results are consistent with those of Ref. 1, and the early point of view that the long-range Coulomb interactions are the driven forces for the ferroelectric states [24].

However, for  $\text{LiBO}_3$ , because the LO modes are soft (i.e.,  $\omega_{LO}^2 < 0$ ), it easy to see from Eq. 7 that  $\omega_s^2$  must also be negative. This suggests that the short-range interactions already favor the symmetry-broken polarized state in these materials. We therefore obtain one of the most



important results of this paper: hyperferroelectrics are a class of ferroelectrics, where the short-range interactions already favorite the symmetry broken polar states. This is a general feature of hyperferroelectrics, or more precisely, a necessary condition for hyperferroelectrics. This could happen in materials, e.g.,  $\text{LiBO}_3$ , where the ions have large size mismatches. Since the hyperferroelectricity comes from short-range local interactions, hyperferroelectrics are not sensitive to the electric boundary conditions. Especially,  $\text{LiOsO}_3$  can be viewed as a special hyperferroelectrics, in which  $\epsilon_\infty \rightarrow \infty$ . More generally, any FE instability in a metal is a limiting case of hyperferroelectric. It is interesting to see if more such metals can be found in searching for novel hyperferroelectrics.

To conclude, we have shown that  $\text{LiBO}_3$  ( $B=\text{V}$ ,  $\text{Nb}$ ,  $\text{Ta}$ ,  $\text{Os}$ ) belong to the recently proposed hyperferroelectrics, despite that some of them ( $\text{LiNbO}_3$  and  $\text{LiTaO}_3$ ) have large band gaps and Born effective charges. By resorting to an effective Hamiltonian model, we clarify that the origin of the hyperferroelectrics is due to the structural instability driven by the short-range interactions. At least one route to find hyperferroelectrics is to search in materials with large ion size mismatches. This work therefore provides a useful guidance in searching for novel hyperferroelectrics.

LH acknowledges valuable discussions with Prof. David Vanderbilt. The work is supported by the Chinese National Science Foundation Grant number 11374275.

---

\* helx@ustc.edu.cn.

- [1] W. Zhong, R. D. King-Smith, and D. Vanderbilt, Phys. Rev. Lett. **72**, 3618 (1994).
- [2] J. Junquera and P. Ghosez, Nature **422**, 506 (2003).
- [3] N. Sai, C. J. Fennie, and A. A. Demkov, Phys. Rev. Lett. **102**, 107601 (2009).
- [4] K. F. Garrity, K. M. Rabe, and D. Vanderbilt, Phys. Rev. Lett. **112**, 127601 (2014).
- [5] J. W. Bennett, K. F. Garrity, K. M. Rabe, and D. Vanderbilt, Phys. Rev. Lett. **109**, 167602 (2012).
- [6] M. J. Polking, M. Han, A. Yourdkhani, V. Petkov, C. F. Kieselowski, V. V. Volkov, Y. Zhu, G. Caruntu, A. P. Alivisatos, and R. Ramesh, Nature Materials **11**, 700 (2012).
- [7] A. F. Penna, A. Chaves, and S. P. S. Porto, Solid State Commun. **19**, 491 (1976).
- [8] Y. Okamoto, P. C. Wang, and J. F. Scott, Phys. Rev. B **32**, 6787 (1985).
- [9] M. S. Zhang and J. F. Scott, Phys. Rev. B **34**, 1880 (1986).
- [10] G. L. Catchen and D. M. Spaar, Phys. Rev. B **44**, 12137 (1991).
- [11] G. Cheng, B. Hennion, P. Launois, M. Xianlin, X. Binchao, and J. Yimin, J. Phys. C **5**, 2707 (1993).
- [12] I. Inbar and R. E. Cohen, Phys. Rev. B **53**, 1193 (1996).
- [13] Y. Shi, Y. Guo, X. Wang, A. J. Princep, D. Khalyavin, P. Manuel, Y. Michiue, A. Sato, K. Tsuda, S. Yu, et al., Nature Materials **12**, 1024 (2013).
- [14] H. J. Xiang, Phys. Rev. B **90**, 094108 (2014).
- [15] H. M. Liu, Y. P. Du, Y. L. Xie, J. M. Liu, C. G. Duan, and X. G. Wan, Phys. Rev. B **91**, 064104 (2015).
- [16] R. M. Pick, M. H. Cohen, and R. M. Martin, Phys. Rev. B **1**, 910 (1970).
- [17] G. Kresse and J. Hafner, Phys. Rev. B **47**, R558 (1993).
- [18] G. Kresse and J. Furthmuller, Phys. Rev. B **54**, 11169 (1996).
- [19] P. E. Blochl, Phys. Rev. B **50**, 17953 (1994).
- [20] A. Togo, F. Oba, and I. Tanaka, Phys. Rev. B **78**, 134106 (2008).
- [21] M. Gajdos, K. Hummer, G. Kresse, J. Furthmuller, and F. Bechstedt, Phys. Rev. B **73**, 045112 (2006).
- [22] C. Thierfelder, S. Sanna, A. Schindlmayr, and W. G. Schmidt, Phys. Status Solidi C **2**, 362 (2010).
- [23] V. Polshettiwar, T. Asefa, and G. Hutchings, Nanocatalysis: Synthesis and Applications p. Fig 14.13 (2013).
- [24] W. Zhong, D. Vanderbilt, and K. M. Rabe, Phys. Rev. B **52**, 6301 (1995).
- [25] M. H. Cohen, Phys. Rev. **99**, 1128 (1955).